Electronic Supplementary Material (ESI) for ChemComm.

Supporting Information

Orthogonal switching of self-sorting processes in a stimuli-responsive library of cucurbit[8]uril complexes

Stefan Schoder, Christoph A. Schalley

Institut für Chemie und Biochemie, Freie Universität Berlin, Takustraße 3, 14195 Berlin, Germany

*** e-mail: c.schalley@fu-berlin.de**

Table of contents

1. Experimental Details

1.1. General Methods

All reagents were commercially available and used without further purification. Thin-layer chromatography (TLC) was performed on aluminum sheets coated with silica gel 60/F254 (Merck KGaA). Column chromatography was performed on silica gel 60 (Merck 40 - 60 nm, 230 - 400 mesh). Melting points were determined on a stuart SMP30 apparatus and are uncorrected. ^{1}H NMR, ^{13}C NMR and ^{1}H, ^{1}H COSY spectra were recorded on Bruker ECX 400 MHz or Bruker AVANCE III 700 MHz NMR spectrometers with a triple inverse cryoprobe on the latter instrument. All chemical shifts are reported in ppm with the residual undeuterated solvents as the internal standards. Coupling constants (J) are given in Hz. UV/Vis spectra were recorded on Varian Cary 50 Bio spectrophotometer. Fluorescence spectra were recorded on a PERKIN ELMER LS50B spectrophotometer. Electrospray-ionization time-of-flight- resolution mass spectrometric (ESI-TOF-HRMS) experiments were conducted on an Agilent 6210 ESI-TOF mass spectrometer. Ethylviologen derivate $EV^{2+}(I^{-})_2$ was prepared according to literature procedure.[1]

1.2. Synthetic procedures.

2-(2-(2-(4-Iodophenoxy)ethoxy)ethoxy)ethan-1-ol (S1)[2]

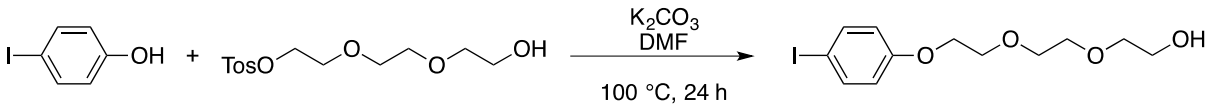

Compound **S1** was prepared according to a modified literature procedure.[2] 4-Iodophenol (1.00 g, 4.55 mmol, 1.0 equiv.), 2-(2-(2-hydroxyethoxy)ethoxy)ethyl 4-methylbenzenesulfonate (1.66 g, 5.46 mmol, 1.2 equiv.) and K_2CO_3 (1.57 g, 11.38 mmol, 2.5 equiv.) were dissolved in DMF (15 mL) and heated to 100 °C for 24 h. The reaction was quenched with a saturated aqueous NH_4Cl solution, extracted with EtOAc (3 x 15 mL) and dried with $MgSO_4$. The crude product was purified by column chromatography (SiO_2, DCM/MeOH = 100:0, 100:1 – 10:1) giving **S1** (1.02 g, 2.90 mmol, 64%) as a yellowish oil. **^{1}H NMR** (400 MHz, $CDCl_3$) δ = 7.53 (d, *J* = 9.1 Hz, 2H, H_d), 6.69 (d, *J* = 9.1 Hz, 2H, H_c), 4.10 – 4.06 (m, 2H, OCH_2), 3.86 – 3.82 (m, 2H, OCH_2), 3.75 – 3.67 (m, 6H, OCH_2), 3.62 – 3.58 (m, 2H, OCH_2) ppm.

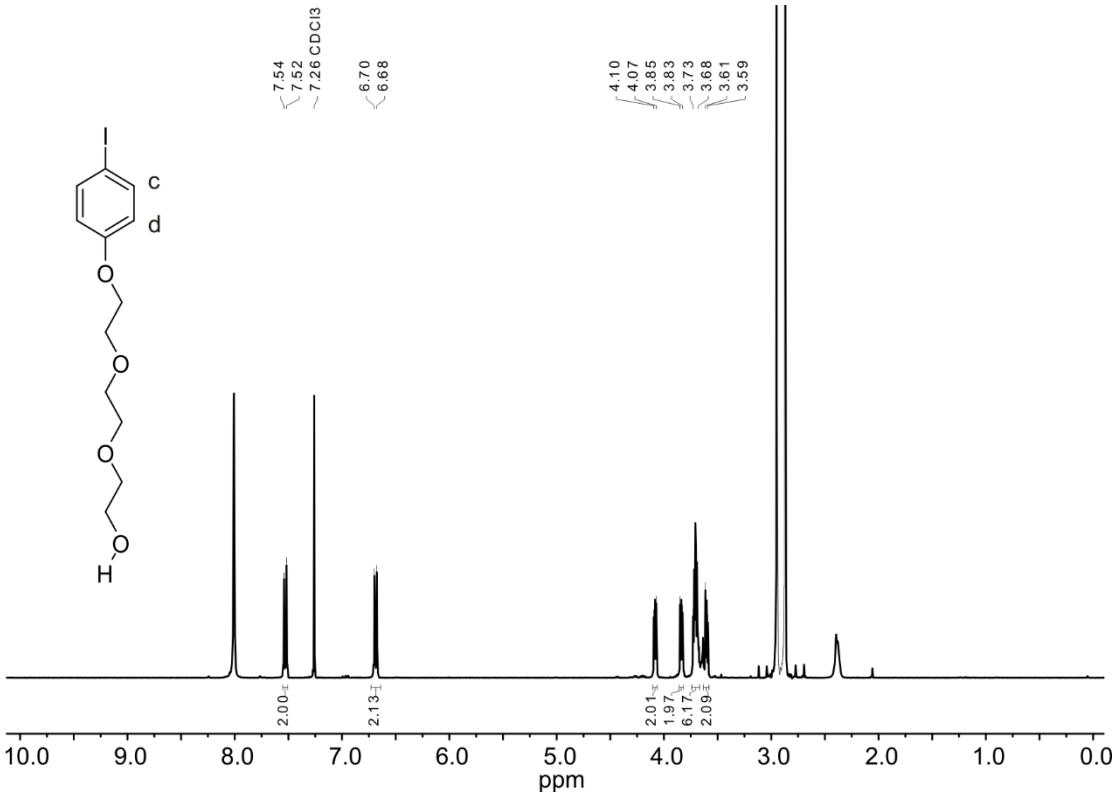

Figure S1. ^{1}H NMR spectrum (400 MHz, $CDCl_3$, 298 K) of **S1**.

2-(2-(2-(4-(Pyridin-4-yl)phenoxy)ethoxy)ethoxy)ethan-1-ol (P)

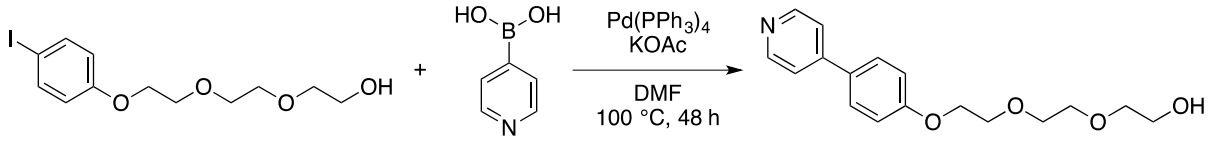

S1 (863 mg, 2.45 mmol, 1.00 eq.), pyridin-4-ylboronic acid (903 mg, 7.35 mmol, 3.00 eq.), $Pd(PPh_3)_4$ (113 mg, 0.49 mmol, 4 mol-%) and KOAc (962 mg, 9.8 mmol, 4.00 eq.) were dissoved in DMF (50 mL) under Ar atmosphere and heated to 100 °C for 48 h. The reaction was quenched with H_2O, extracted with EtOAc (3 x 50 mL), filtered over celite, washed with NaCl aq. (1 x 25 mL) and dried with $MgSO_4$. The crude product was purified by column chromatography (SiO_2, DCM/MeOH = 150:0, 150:1 – 15:1) giving **P** (153 mg, 0.50 mmol, 21%) as a colourless powder. **^{1}H NMR** (700 MHz, D_2O) δ 8.68 (d, *J* = 6.9 Hz, 2H, H_a), 8.25 (d, *J* = 7.0 Hz, 2H, H_b), 7.95 (d, *J* = 8.8 Hz, 2H, H_c), 7.21 (d, *J* = 8.8 Hz, 2H, H_d), 4.34 – 4.31 (m, 2H, OCH_2), 3.96 – 3.94 (m, 2H, OCH_2), 3.80 – 3.78 (m, 2H, OCH_2), 3.74 – 3.72 (m, 2H, OCH_2), 3.72 – 3.70 (m, 2H, OCH_2), 3.65 – 3.62 (m, 2H, OCH_2) ppm. **^{13}C NMR** (176 MHz, Deuterium Oxide) δ 161.41, 157.27, 140.60, 129.87, 126.93, 123.23, 115.68, 71.67, 69.81, 69.41, 68.92, 67.26, 60.32 ppm. ESI-TOF-HRMS: *m/z* calcd for $[C_{17}H_{21}NO_4+H]^+$ 304.1543, found 304.1565; calcd for $[C_{17}H_{21}NO_4+Na]^+$ $C_{17}H_{21}NO_4$ 326.1363, found 326.1353. M.p. 110.2 – 110.7 °C.

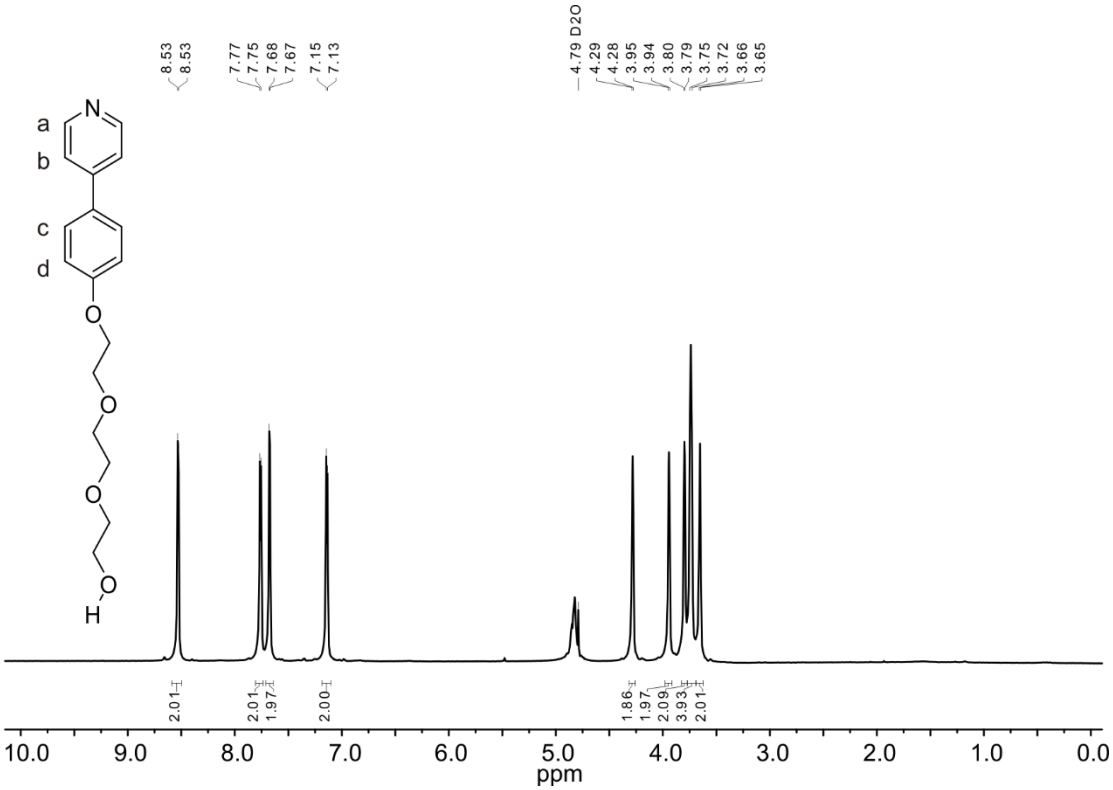

Figure S2. ^{1}H NMR spectrum (700 MHz, D_2O, 298 K) of **P**.

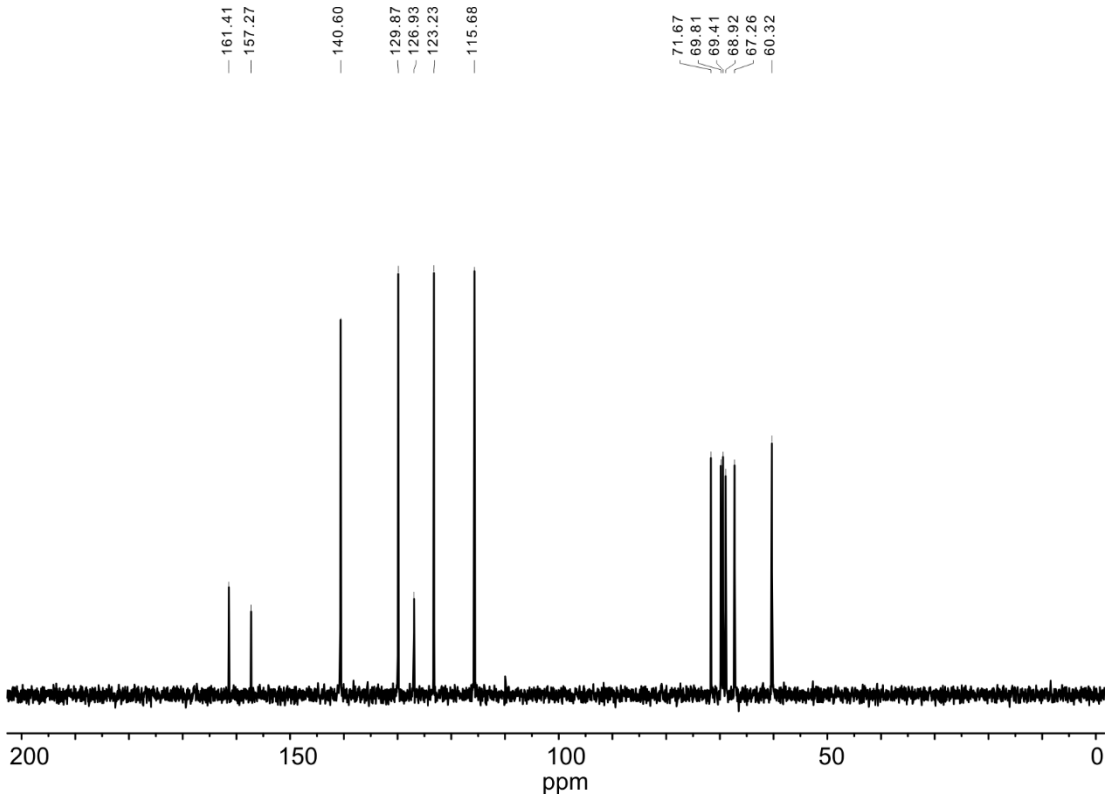

Figure S3. ^{13}C NMR spectrum (176 MHz, D_2O, 298 K) of **P**.

2,2'-(((((Naphthalene-2,6-diylbis(oxy))bis(ethane-2,1-diyl))bis(oxy))bis(ethane-2,1-diyl))bis(oxy))bis(ethan-1-ol) (N)[3]

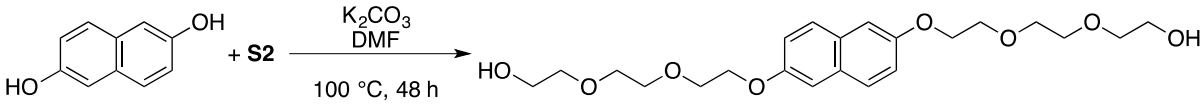

Compound **N** was prepared according to a modified literature procedure.[3] 2,6-Dihydroxynaphthalene (500 mg, 3.12 mmol, 1.0 eq.), 2-(2-(2-hydroxyethoxy)ethoxy)ethyl 4-methylbenzenesulfonate (2.48 g, 7.80 mmol, 2.5 eq.) and K_2CO_3 (2.18 g, 15.6 mmol, 5.0 eq.) were dissolved in DMF (15 mL) and heated to 100 °C for 48 h. The reaction was quenched with H_2O, extracted with EtOAc (3 x 15 mL), washed with NaCl aq. (1 x 15 mL) and dried with $MgSO_4$. The crude product was purified by column chromatography (SiO_2, DCM/MeOH = 100:0, 100:1 – 10:1) giving **N** (303 mg, 0.713 mmol, 23%) as a colourless powder. **^{1}H NMR** (700 MHz, D_2O) δ 7.83 (d, *J* = 8.9 Hz, 2H, , H_y), 7.40 (d, *J* = 2.5 Hz, 2H, H_z), 7.28 (dd, *J* = 8.9, 2.5 Hz, 2H, H_x), 4.38 – 4.33 (m, 4H, OCH_2), 4.00 – 3.96 (m, 4H, OCH_2), 3.83 – 3.79 (m, 4H, OCH_2), 3.77 – 3.73 (m, 4H, OCH_2), 3.74 – 3.70 (m, 4H, OCH_2), 3.67 – 3.63 (m, 4H, OCH_2) ppm.

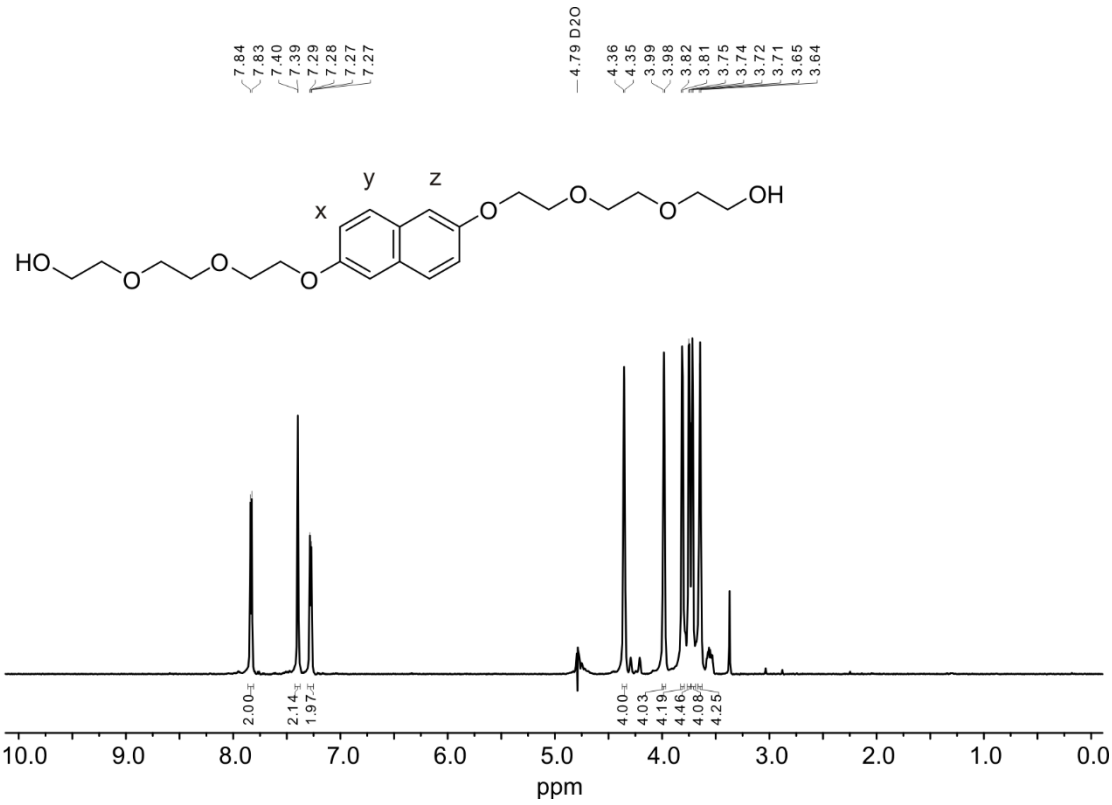

Figure S4. ^{1}H NMR spectrum (700 MHz, D_2O, 298 K) of **N**.

2. NMR, UV/Vis, Mass and Fluorescence Experiments Complementary to those in the Main Text

2.1. ^{1}H NMR signal assignment for complex $(PH^+)_2$@Q

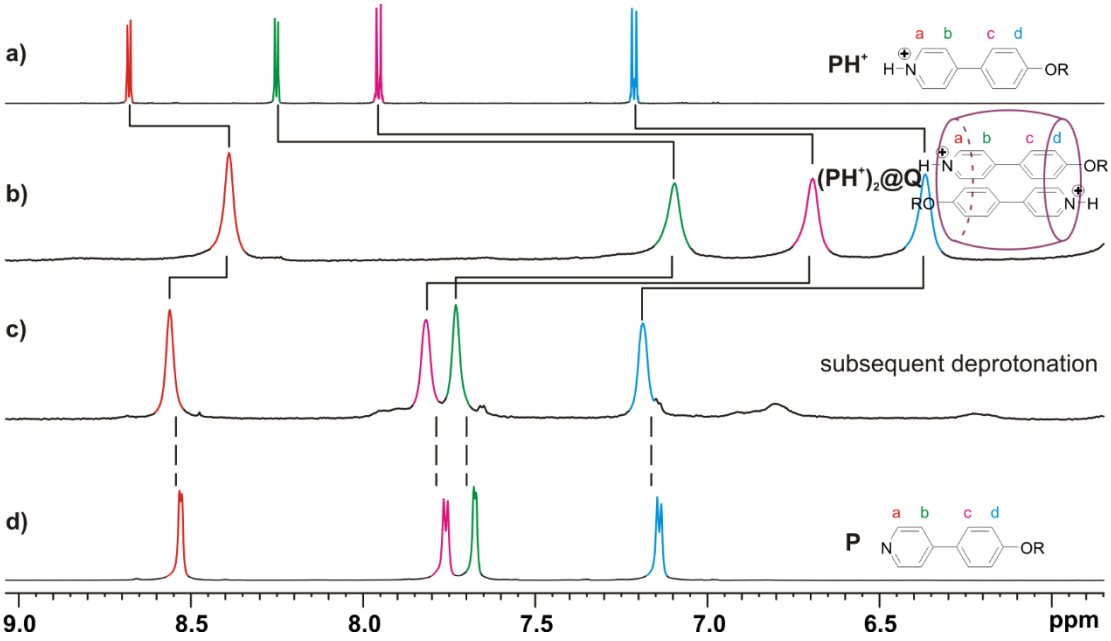

Figure S5. Partial ^{1}H NMR spectra (700 MHz, 298 K, D_2O, 1.0 mM) of the compounds depicted. a) **PH$^+$** (pH 4), b) a 2:1 mixture of **PH$^+$** and **Q** in acidic (pH 4) and c) basic (pH 10) medium, d) **P** (pH 10). The high-field shift of all four protons in the cucurbituril complex (a to b) indicate that the guest is fully threaded in the host and - in accordance with literature reports[4] - forms the 2:1 complex (**PH$^+$)$_2$@Q**. Subsequent deprotonation (c) results in the NMR of deprotonated compound **P** (d) indicating the complete dissociation of the complex. DCl (35% in D_2O) and K_2CO_3 were used to (de)protonate.

2.2. Reversibility of the formation of $(PH^+)_2$@Q

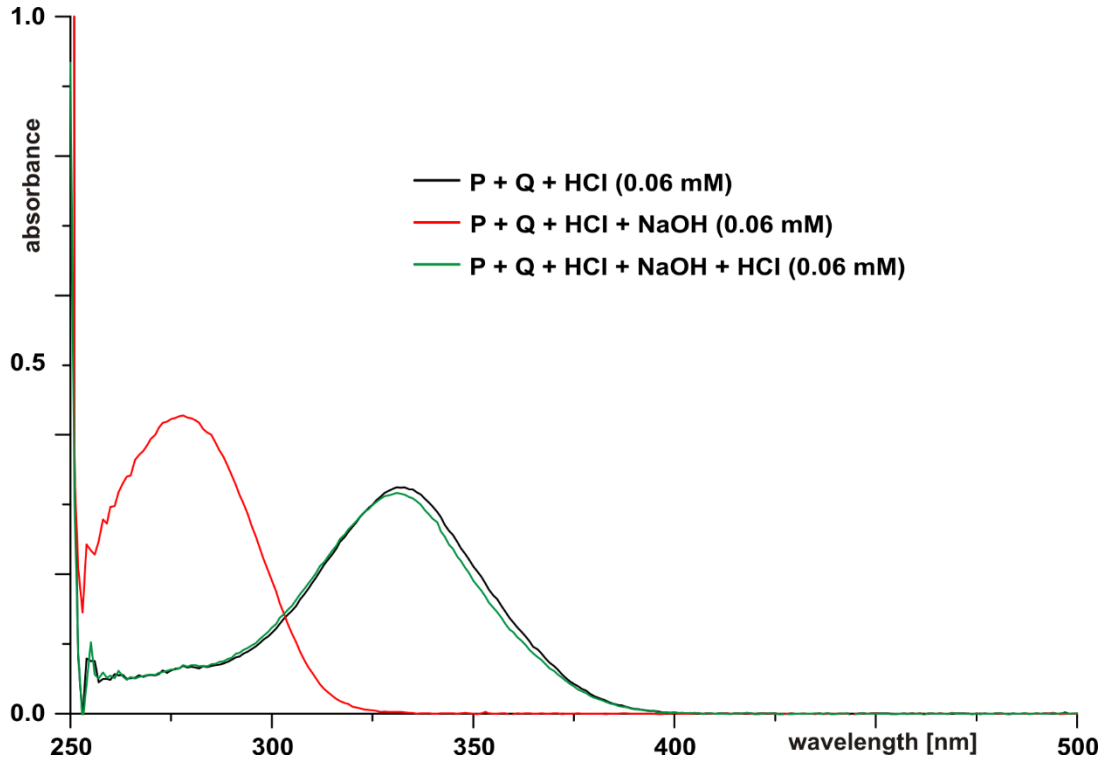

Figure S6. UV/Vis spectra of a 0.06 mM solution of **$(PH^+)_2$@Q** (black line), after deprotonation (red line) and after subsequent protonation (green line). Recovery of the original band after the protonation indicates the reversibility of the formation of **$(PH^+)_2$@Q**.

2.3. Fluorescence spectra of P, PH^+ and $(PH^+)_2$@Q

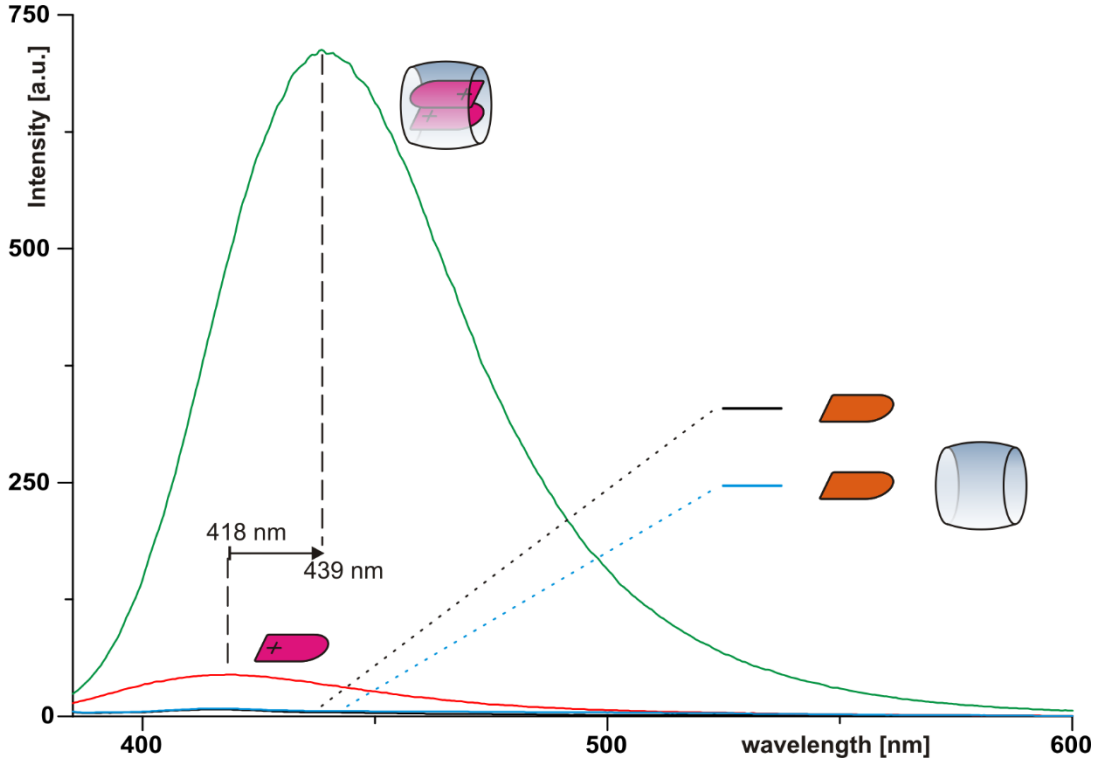

Figure S7. Fluorescence spectra of **P**, **PH^+**, **$(PH^+)_2$@Q** and a mixture of **P** and **Q** all at the same concentration; excitation at 366 nm. The fluorescence red shift and the remarkable increase of the 2:1 complex **$(PH^+)_2$@Q** are in line with similar phenylpyridinium derivates.[5] Unprotonated **P** is not emitting and consequently a mixture of **P** and **Q** is neither.

2.4. Determination of the association constant with ITC

ITC titration experiment was carried out on a VP-ITC from Microcal Inc. at 25 °C in a 60 mM phosphate buffer (pH=5). The host was in the sample cell at a concentration of 0.03 mM, and the guest was in the syringe at a concentration of 1.0 mM. A titration consisted of 30 consecutive injections of 2-10 µL with at least 250 s intervals between injections. The first data point was removed from the data set prior to curve fitting. Heats of dilution were checked by titration well beyond saturation or by titration of the guest into a buffer solution and subtracted from the normalized enthalpies. The data were analyzed with Origin 7.0 software, using the sequential binding sites model. The binding constant was calculated as an average of several experiments.

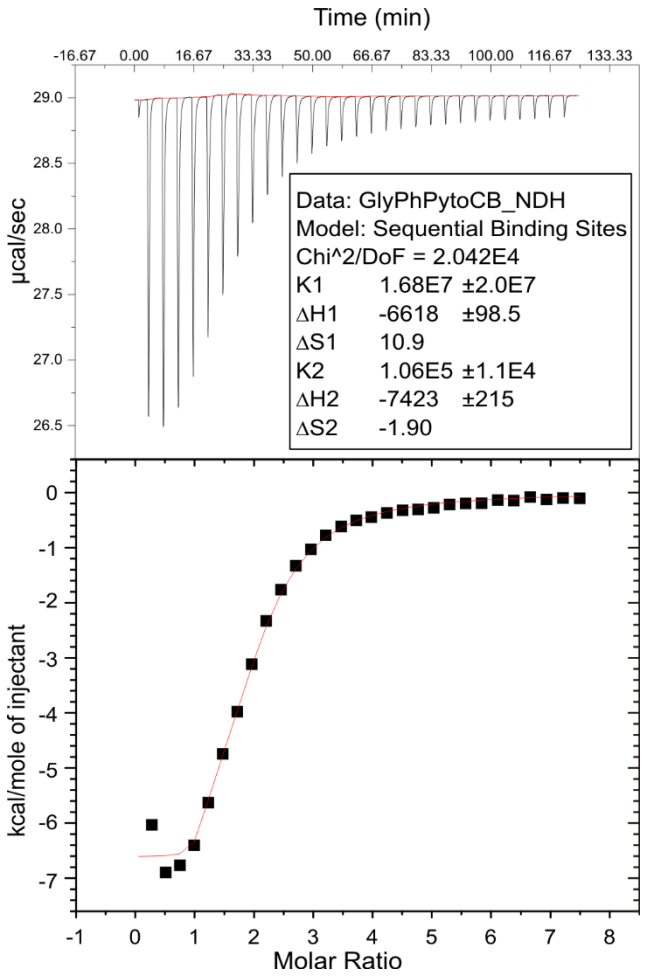

Figure S8. ITC data for the titration of **Q** (0.03 mM) with $\mathbf{PH^+}$ (1.0 mM) in a 60 mM phosphate buffer (pH=5) at 25 °C. ΔH_1 = -6618 cal/mole, ΔS_1 = 10.9 cal/mole*K, ΔG_1 = -9867 cal/mole; ΔH_2 = -7423 cal/mole, ΔS_2 = -1.9 cal/mole*K, ΔG_2 = -6857 cal/mole.

2.5. Mass spectrum of $(PH^+)_2$@Q

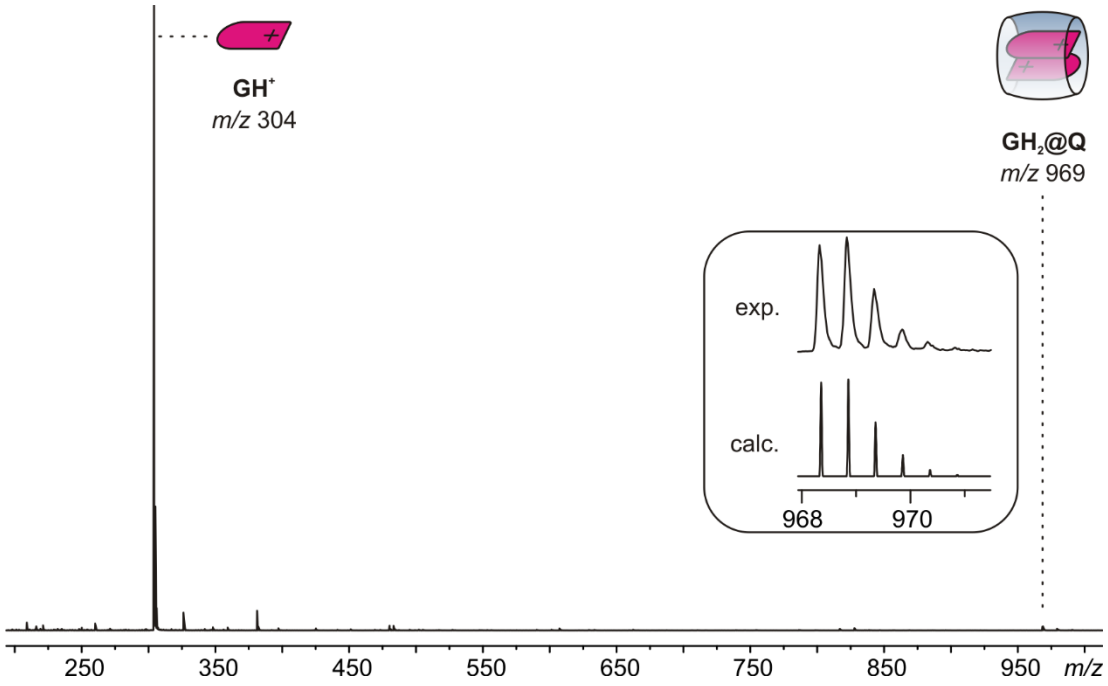

Figure S9. ESI-TOF mass spectrum of a mixture of **PH^+** and **Q**. This signal of **$(PH^+)_2$@Q** is not very intense as charge repulsion leads to quick fragmentation in the gas phase. Because of the used settings of the instrument the signal for the 1:1 complex **PH^+@Q** cannot be seen.

2.6. ^{1}H NMR signal assignment for complex PH$^+$N@Q

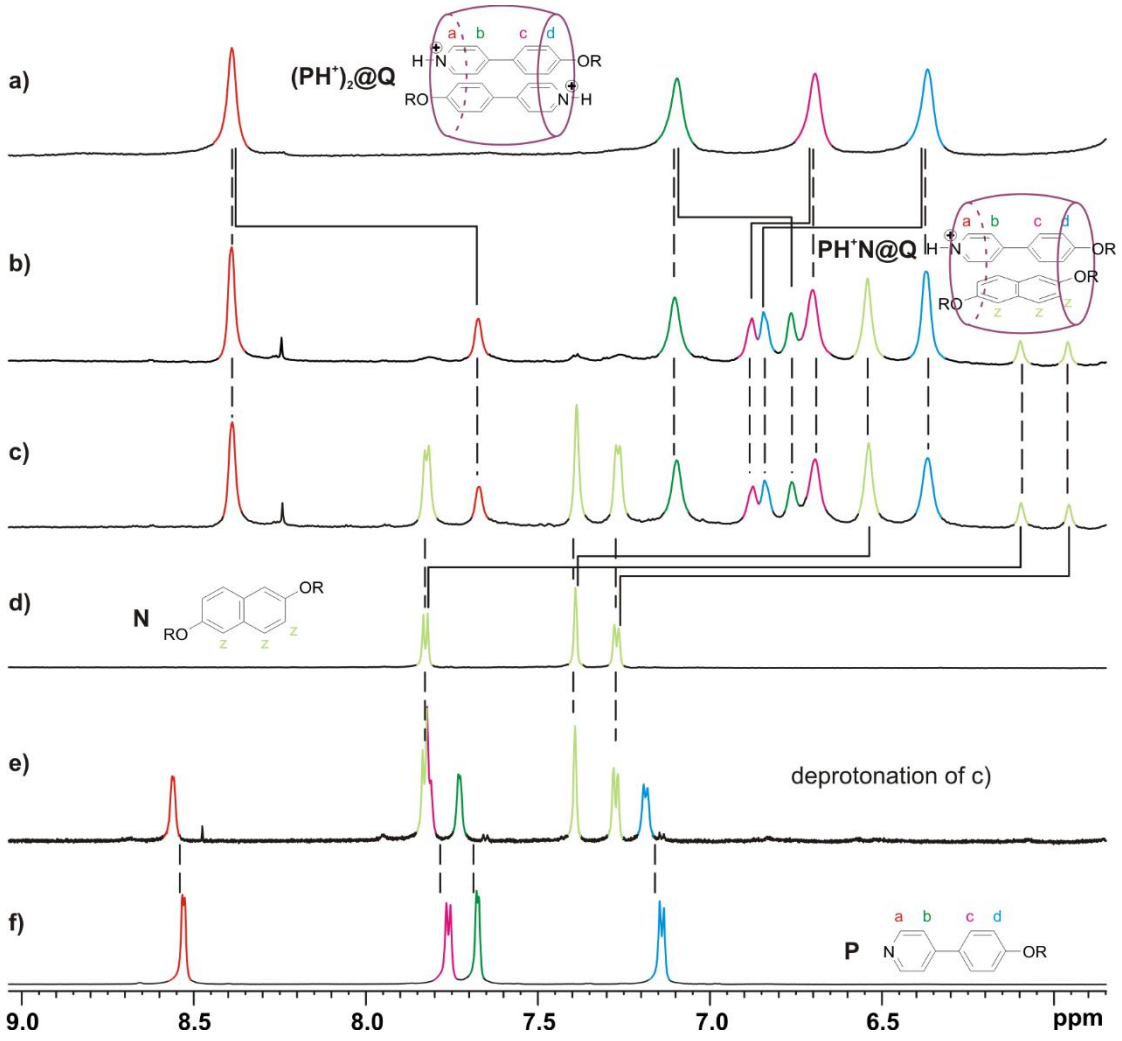

Figure S7. Partial ^{1}H NMR spectra (700 MHz, 298 K, D_2O, 1.0 mM) of a) **(PH$^+$)$_2$@Q** (pH 4), b) a 3:1:2 mixture of **PH$^+$**, **N** and **Q** in acidic (pH 4) medium c) an equimolar mixture of **PH$^+$**, **N** and **Q** in acidic (pH 4) medium, d) **N**, e) an equimolar mixture of **P**, **N** and **Q** in basic (pH 10) medium, f) **P** (pH 4). DCl (35% in D_2O) and K_2CO_3 were used to (de)protonate. Addition of **N** to complex **(PH$^+$)$_2$@Q** results in the formation of a new complex. Spectrum b) shows a mixture of the two complexes **(PH$^+$)$_2$@Q** and **PH$^+$N@Q** in a 1:1 stoichiometry coming from a 3:1:2 mixture of **PH$^+$**, **N** and **Q**. If the guests and the host are in a 1:1:1 mixture (spectrum c) the 1:1:1 complex **PH$^+$N@Q** does not form exclusively. The ration between the two complexes cannot be predicted, resulting in signals for the unbound free **N**. This leads to the assumption, that the binding constants of the inclusion of the second guest are similar. Deprotonation (spectrum e) of **PH$^+$** in the 1:1:1 mixture of spectrum c) leads in the superposition of the signals of the free guests **P** and **N** indicating the dissociation of the complexes.

2.7. ^{1}H NMR spectrum of V^{2+}N@Q

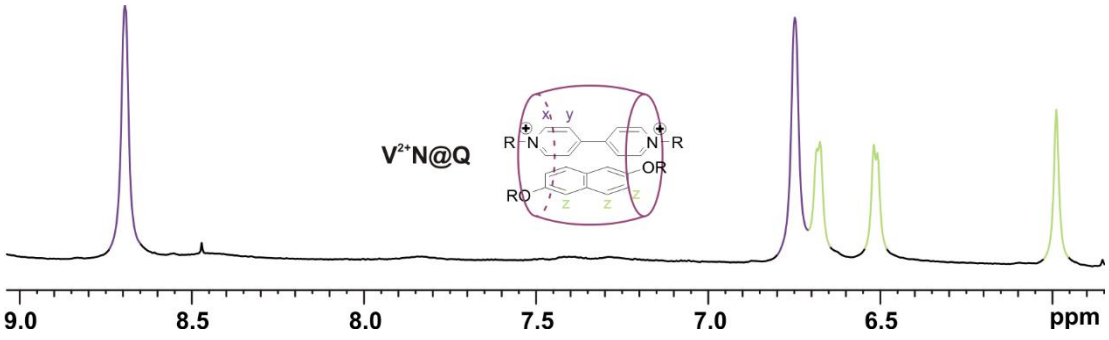

Figure S8. Partial ^{1}H NMR spectrum (700 MHz, 298 K, D_2O, 1.0 mM) of **V^{2+}N@Q** with strong high field shifts of the signals of the protons on **N** similar to a literature-known complex.[6]

2.8. ^{1}H NMR signal assignment for complex PV^{2+}@Q

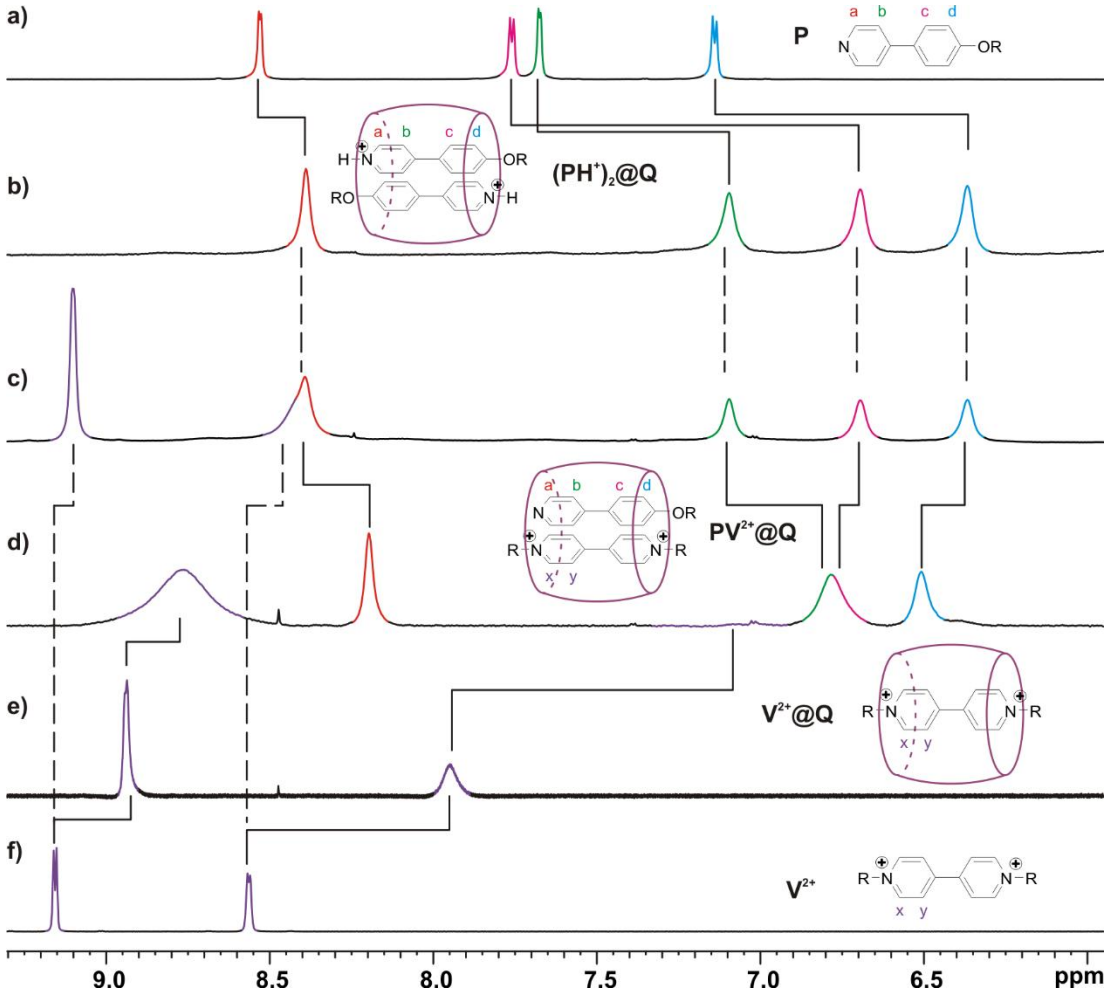

Figure S12. Partial ^{1}H NMR spectra (700 MHz, 298 K, D_2O, 1.0 mM) of (a) **P** (pH 10), (b) **$(PH^+)_2$@Q** (pH 4), (c) a 2:1:1 mixture of **PH^+**, **V^{2+}** and **Q** in acidic (pH 4) medium resulting in the formation of **$(PH^+)_2$@Q** and free **V^{2+}** (pH 4), (d) a 1:1:1 mixture of **P**, **V^{2+}** and **Q** in basic (pH 10) medium resulting in the formation of **PV^{2+}@Q**, (e) complex **V^{2+}@Q** and (f) **V^{2+}**. DCl (35% in D_2O) and K_2CO_3 were used to (de)protonate. Spectrum c) shows that the formation of complex **$(PH^+)_2$@Q** is favored over the formation of complex **V^{2+}@Q** due to the higher binding constant of the 2:1 complex. After deprotonation of **PH^+** (spectrum d) a new complex is formed including **P**, **V** and **Q** which can be attributed to the pi-donor-pi-acceptor complex **PV^{2+}@Q**.

2.9. Structural assignment of PV^{2+}@Q

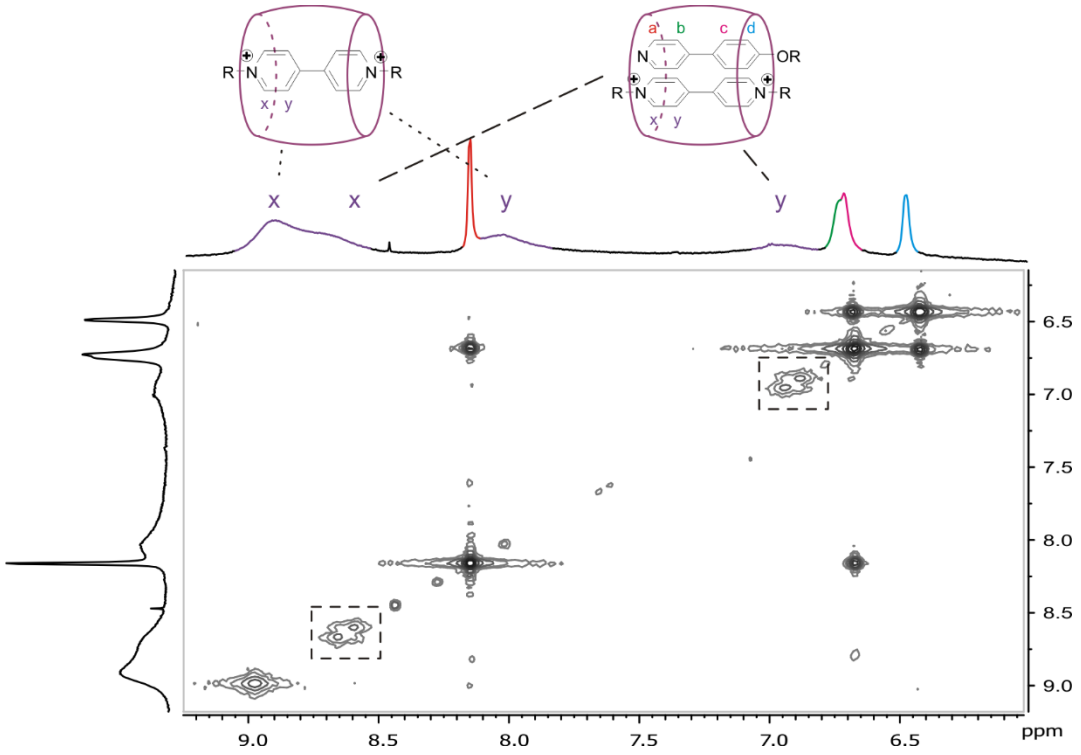

Figure S13. Partial ^{1}H ^{1}H COSY NMR spectra (700 MHz, 278 K, D_2O, 1.0 mM) of a 1:1:1 mixture of **P**, $\mathbf{V^{2+}}$ and **Q** in basic conditions. The signals for the complex $\mathbf{V^{2+}}$**@Q** are known and ca be assigned. Because of the low solubility of the complex and because of the shielding of the cucurbituril the cross peaks for the complex cannot be seen. The new set of signals (marked with dashed squares) are attributed to the new viologen containing complex $\mathbf{PV^{2+}}$**@Q**. The viologen experiences the same shielding resulting in no visible cross peaks at this low concentration.

2.10. Reversibility of the formation of PV^{2+}@Q

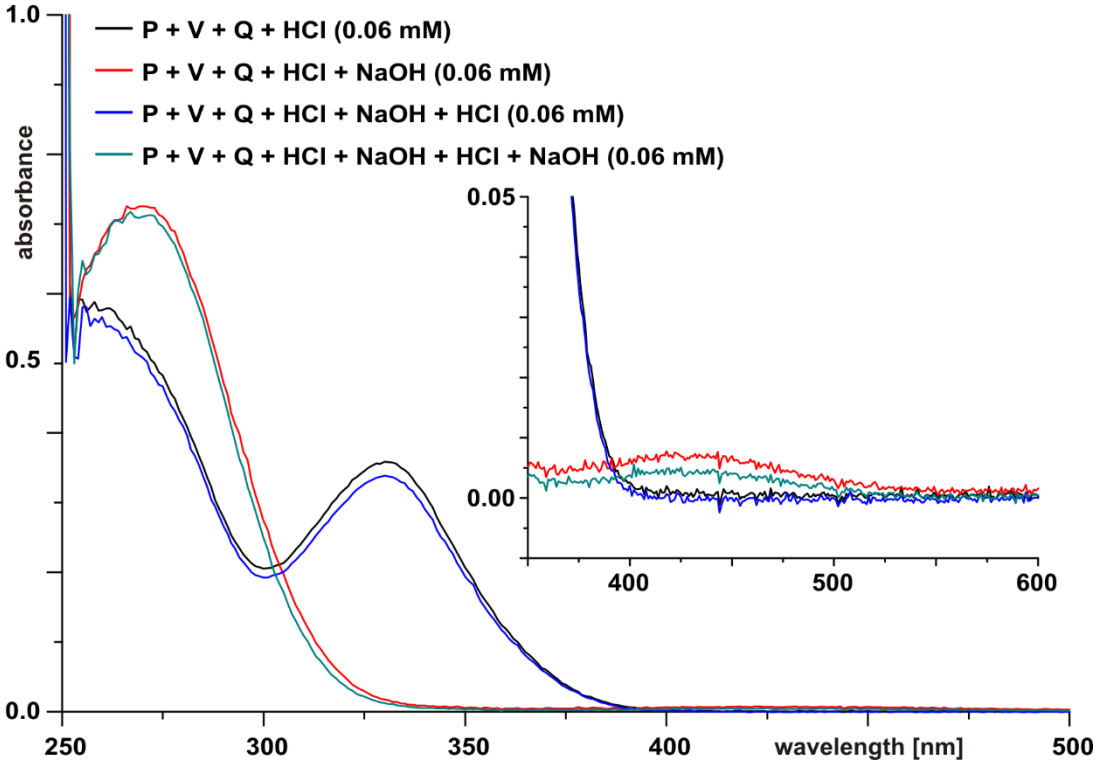

Figure S14. UV/Vis spectra of a 1:1:1 mixture of **PH^+**, **V^{2+}** and **Q** in acidic conditions (black line), after deprotonation (red line), after consecutive protonation (blue line) and subsequent deprotonation (cyan line) (6 µM **V^{2+}**). In acidic conditions the absorption maximum corresponds to the complex **$(PH^+)_2$@Q**. Inlay shows the chargte-transfer band of the formed complex **PV^{2+}@Q**. Recovery of the original band after the protonation indicates the reversibility of the formation of the complex.

2.11. Cyclic voltrammetry

Redox-potentials reported in this study were obtained by cyclic voltammetry. Measurements were carried out in aqueous solutions with 0.1 M electrolyte and 1 mM analyte concentration using a three-electrode configuration (glassy carbon working electrodes, Pt counter electrode, Ag wire as pseudoreference) and an Autolab PGSTAT302N potentiostat. The decamethylferrocene/ decamethylferrocenium ($[FeCp_2^*]^{+/0}$) couple was used as the internal reference for all measurements to ensure maximum comparability. Energy differences were calculated according to the equation $\Delta G = -n\,F\,\Delta E$.

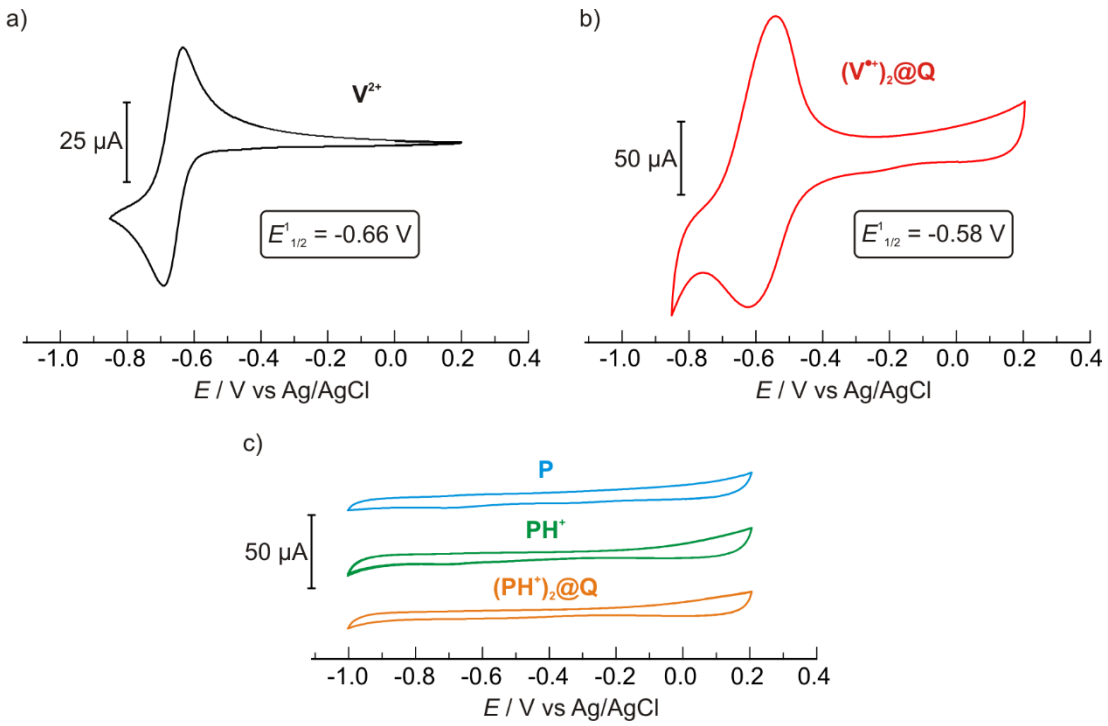

Figure S95. Cyclic voltammetry measurements of a) $\mathbf{V^{2+}}$, b) $\mathbf{(V^{\bullet+})_2@Q}$ and c) measurements of **P**, $\mathbf{PH^+}$ and $\mathbf{(PH^+)_2@Q}$.

2.12. Formation of the complex $(V^{\bullet+})_2$@Q

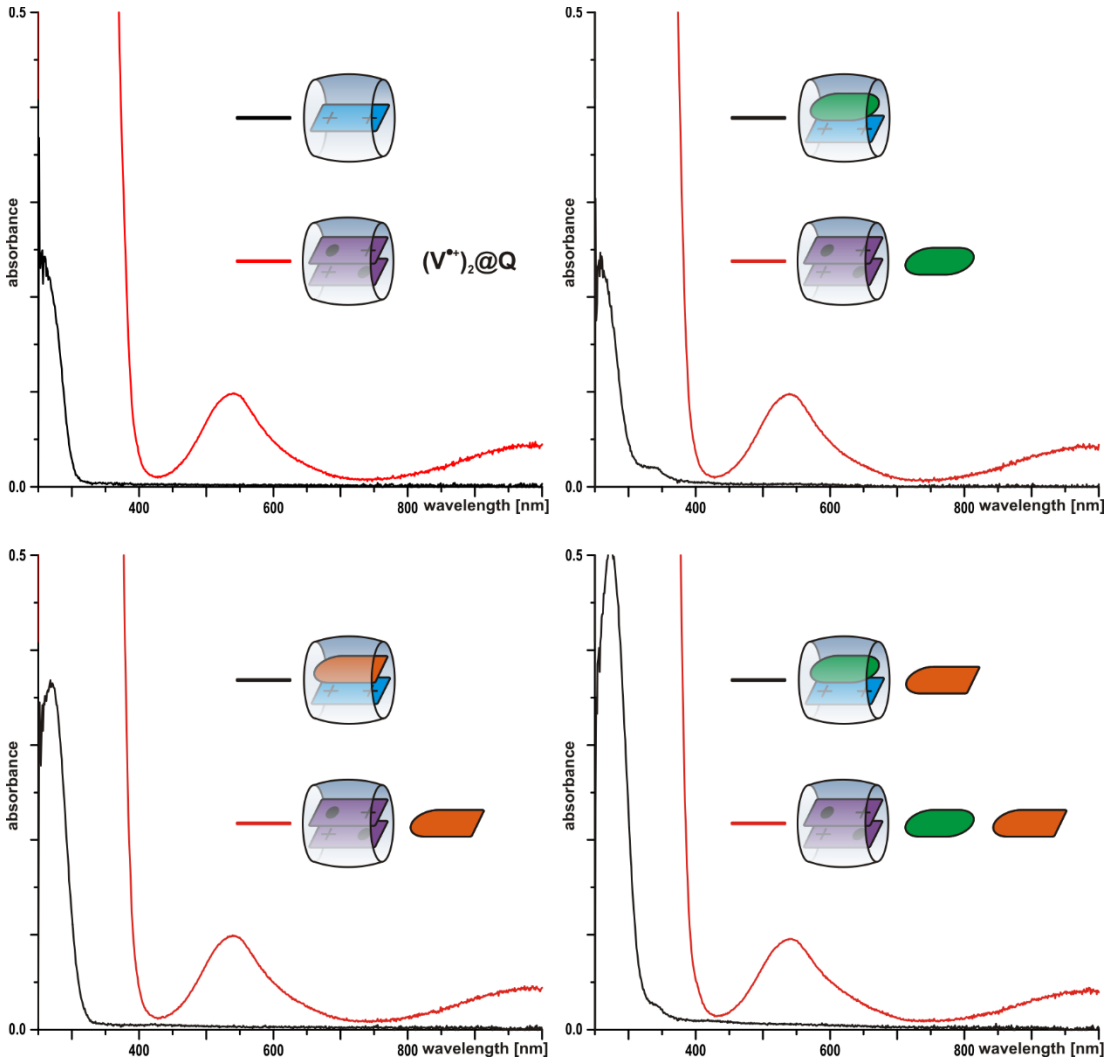

Figure S16. UV/Vis spectra of the shown complexes before (top structures) and after reduction (bottom structures) with $Na_2S_2O_4$. In all mixtures reduction leads to the formation of the complex **$(V^{\bullet+})_2$@Q**.

2.13. ^{1}H NMR signal assignment for a four-step square network

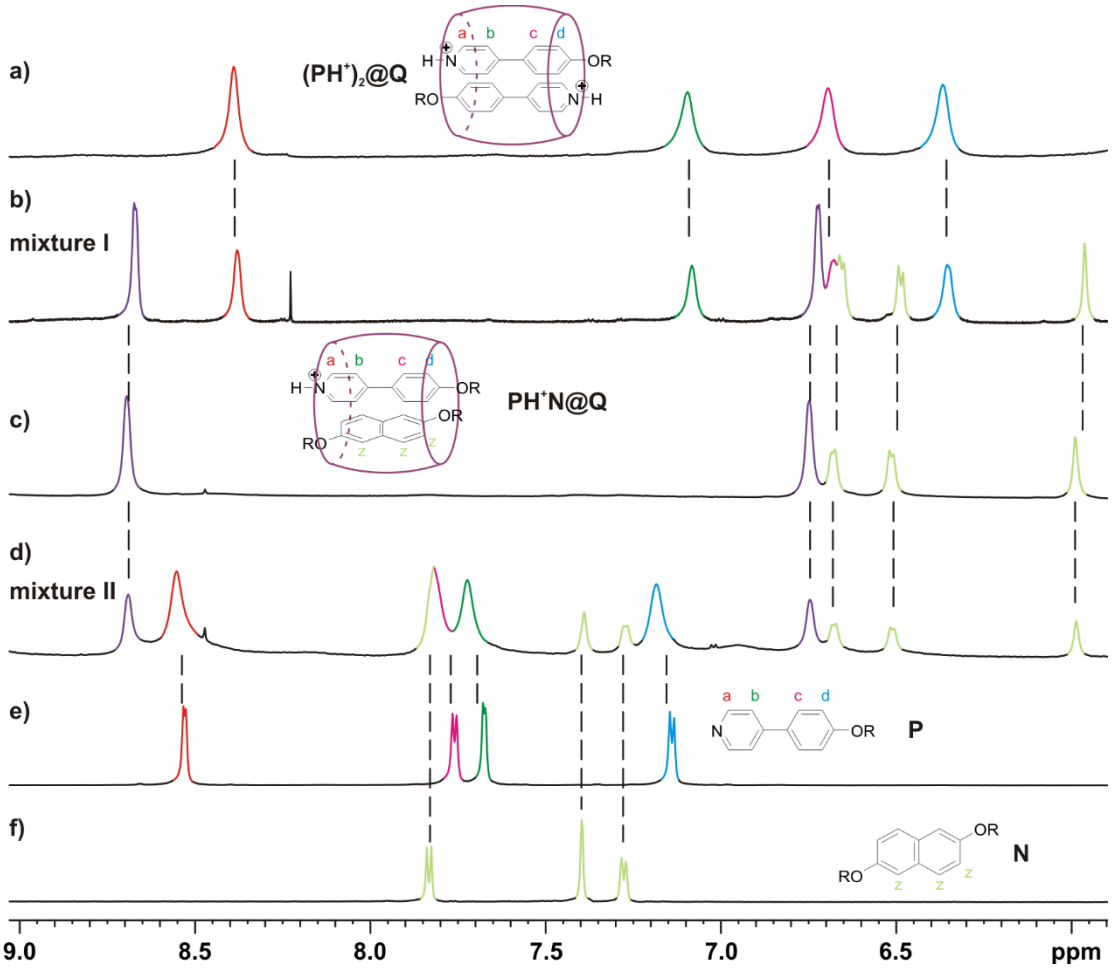

igure S17. Partial ^{1}H NMR spectra (700 MHz, 298 K, D_2O, 1.0 mM) of (a) **$(PH^+)_2$@Q**, (b) mixture **I**, a 2:1:1:2 mixture of **PH^+**, **V^{2+}**, **N** and **Q** in acidic (pH 4) medium, (c) **V^{2+}N@Q**, (d) mixture **II**, a 2:1:1:2 mixture of **P**, **V^{2+}**, **N** and **Q** in basic (pH 10) medium, (e) **P** (pH 10) and (f) **N**. Spectrum b) shows the signals for the two complexes **$(PH^+)_2$@Q** and **V^{2+}N@Q** and resembles **state I**. Subsequent deprotonation of **PH^+** (spectrum d) shows the signal for complex **V^{2+}N@Q** and free **P** indicating the dissociation of the complex **$(PH^+)_2$@Q** and therefore resembling **state II**. To avoid formation of **PV^{2+}@Q** a slight excess of **N** was used, resulting in a set of signals for free **N**.

2.14. Control experiment of state I and II regarding $Na_2S_2O_4$

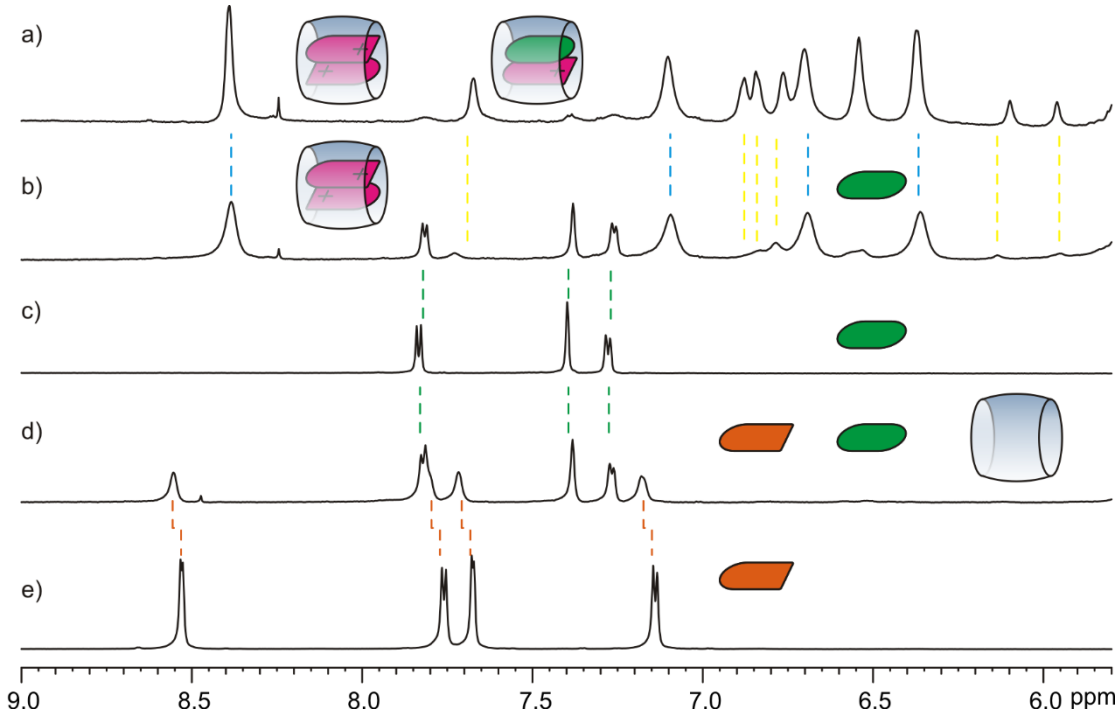

Figure S18. Partial ^{1}H NMR spectra (700 MHz, 298 K, D_2O, 1.0 mM) of a) a 2:1:2 mixture of **PH$^+$**, **N** and **Q** in acidic (pH 4) medium (corresponding to state **I** without **V^{2+}**), b) the same solution after addition of $Na_2S_2O_4$, c) **N**, d) a 2:1:2 mixture of **P**, **N** and **Q** in basic (pH 10) medium (corresponding to state **II** without **V^{2+}**) after addition of $Na_2S_2O_4$, e) **P** (pH 10). Addition of reductant to the acidic mixture (a to b) does not result in the formation of a new complex. Therefore, the reaction mixture is not affected by the addition of $Na_2S_2O_4$. The same holds true under basic conditions (d) which is a superposition of the signals of the free guests.

2.15. Reduction of state I

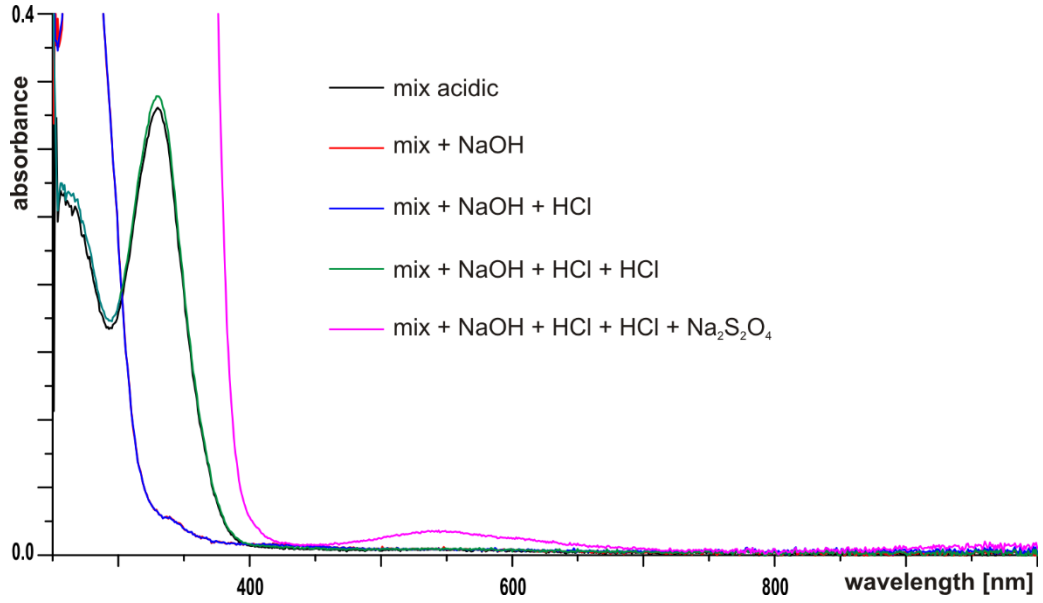

Figure S19. This UV/Vis experiment shows the reduction of state **I** (an acidic mixture) to state **IV** (a reduced state in acidic medium). Because of the fast reoxidation of viologen in acidic medium a solution mixture should be prepared which is just slightly acidic. The black line corresponds to a 2:1:1:2 mixture of **PH$^+$**, **V^{2+}**, **N** and **Q** in H_2O (24 µM **V^{2+}**). It should be noted that due to solubility reasons the solution is slightly acidic. To assure just a slightly acidic solution the original mixture (black line) was deprotonated with 2 µL 1.5M NaOH (red line; lying under the blue line) and slowly acidified. After the first addition of 1.4 µL of 1M HCl (blue) the solution is still basic. After the second addition of 1.4 µL of 1M HCl (green) the solution is acidic reperesenting state **I**. Reduction with $Na_2S_2O_4$ (pink line) results in the expected absorption maxima of state **IV**. The intensity of the signal is weak, because of the fast reoxitation while the measurement.

2.16. Acidification of state III

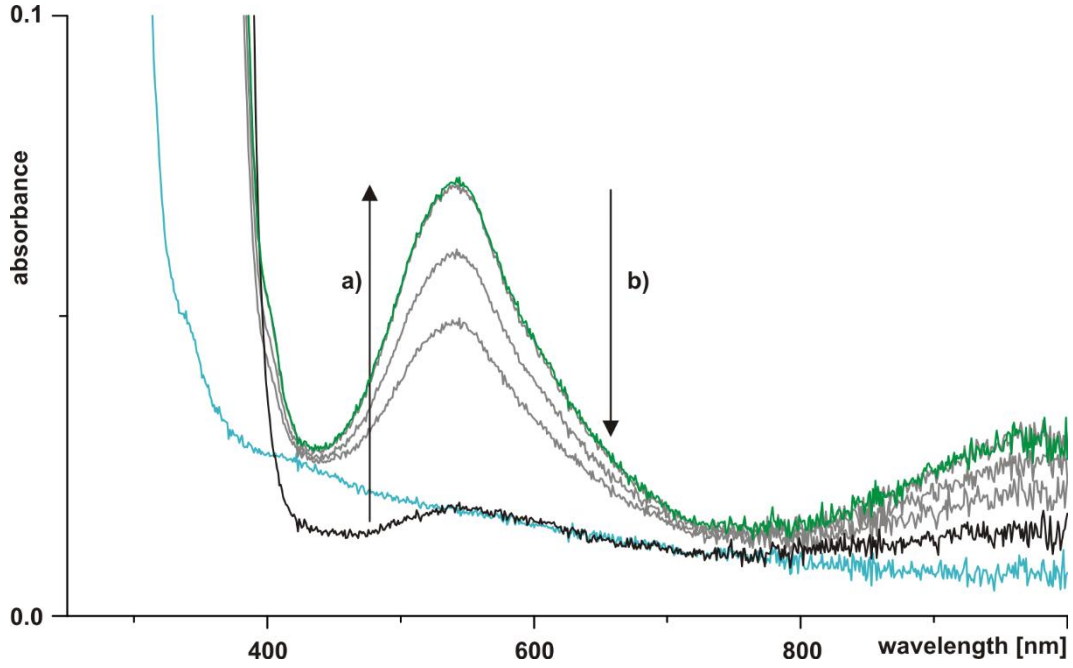

Figure S20. This UV/Vis experiment shows the acidification of state **III** (a reduced state in basic medium) to state **IV** (a reduced state in acidic medium). The black line corresponds to a 2:1:1:2 mixture of **P**, $\mathbf{V^{2+}}$, **N** and **Q** in H_2O (24 µM $\mathbf{V^{2+}}$) after addition of 1 µL 1.5M NaOH (black line). It should be noted that due to solubility reasons the solution was slightly acidic before. Reduction with $Na_2S_2O_4$ (green line) results in the expected absorption maxima of state **III** (depicted by arrow a). After addition of 1.4 µL 1M HCl (b) (grey lines) state **IV** is reached. The absorption maxima decreases rapidly (arrow b) because of reoxidation resulting in the reoxidised state (blue line) within 2 minutes.

References

1. L. Cera and C. A. Schalley, *Chem. Sci.*, 2014, **5**, 2560-2567.
2. W. Qu, M.-P. Kung, C. Hou, S. Oya and H. F. Kung, *J. Med.Chem.*, 2007, **50**, 3380-3387.
3. Y. Han, J.-B. Guo, J. Cao and C.-F. Chen, *Tetrahedron*, 2013, **69**, 4541-4545.
4. S. Senler, L. Cui, A. M. Broomes, E. L. Smith, J. N. Wilson and A. E. Kaifer, *J. Phys. Org. Chem.*, 2012, **25**, 592-596.
5. Y. Zhang, T.-Y. Zhou, K.-D. Zhang, J.-L. Dai, Y.-Y. Zhu and X. Zhao, *Chem. Asian J.*, 2014, **9**, 1530-1534.
6. H.-J. Kim, J. Heo, W. S. Jeon, E. Lee, J. Kim, S. Sakamoto, K. Yamaguchi and K. Kim, *Angew. Chem. Int. Ed.*, 2001, **40**, 1526-1529.